International Journal of Quantum Information
Vol. 12, Nos. 7 & 8 (2014) 1560019 (15 pages)

DOI: 10.1142/S0219749915600199

Phase randomization and typicality in the interference of two condensates

Paolo Facchi[*,†], Hiromichi Nakazato[‡], Saverio Pascazio[*,†,§], Francesco V. Pepe[*,†], Golam Ali Sekh[†] and Kazuya Yuasa[‡]

[*]*Dipartimento di Fisica and MECENAS, Università di Bari, I-70126 Bari, Italy*

[†]*INFN, Sezione di Bari, I-70126 Bari, Italy*

[‡]*Department of Physics, Waseda University, Tokyo 169-8555, Japan*

Received 7 October 2014
Accepted 24 November 2014
Published 5 February 2015

Interference is observed when two independent Bose–Einstein condensates expand and overlap. This phenomenon is typical, in the sense that the overwhelming majority of wave functions of the condensates, uniformly sampled out of a suitable portion of the total Hilbert space, display interference with maximal visibility. We focus here on the phases of the condensates and their (pseudo) randomization, which naturally emerges when two-body scattering processes are considered. Relationship to typicality is discussed and analyzed.

Keywords: Interference; Bose–Einstein condensates; typicality; randomness.

1. Introduction

The physical significance of the phase of a Bose–Einstein condensate (BEC) has raised a number of interesting foundamental quantum-mechanical questions.[1–7] Interference is observed even when two condensates are prepared *independently*.[8] This phenomenon, characteristic of condensates, contrasts with common wisdom on single-particle double-slit interference experiments,[9,10] where no interference can be observed unless the relative phase between the two branch waves is kept constant.[11,12] In this sense, independent sources do not interfere (at first order; the second-order Hanbury Brown and Twiss interference[13–15] is a different story).

The most credited explanation of the observation of interference in two-mode Bose systems relies on the beautiful idea that the relative phase of the condensates is established by measurement. The phase offset of each single interference pattern

[§]Corresponding author.

changes from run to run, so that no interference persists if many interference patterns are superimposed: There is thus no contradiction with the standard quantum-mechanical interpretation of first-order interference. This "measurement-induced interference" was first proposed in Ref. 16 and then corroborated by a number of studies.[17–21] The interpretation of the experimental results has also been formalized in terms of positive operator valued measures.[22,23] These ideas bear consequences on our understanding of symmetry breaking phenomena.[2,5,7,24]

We showed in Ref. 25 that interference is robust with respect to the state preparation. Each time two condensates are experimentally prepared (e.g. out of a single condensate, by inserting a "wall" between them[8,26–30]), their wave function is sampled out of a portion of the total Hilbert space that depends on experimental procedures and details (state preparation). Since we have no access to this information, we have to look at the *typical* features of such a wave function, namely those features that characterize its behavior and properties in the overwhelming majority of cases. We find that the very presence of an interference pattern emerges as a typical feature of the wave function.[25]

In this paper we will build on this observation and focus on phase randomization effects due to self-interaction within the condensate, to clarify how the phase randomization process can take place. This paper is organized as follows. In Sec. 2, we introduce the ensemble of initial states and review its properties. In particular, we define and analyze the averages and variances of the physical observables. Section 3 is devoted to the study of the general properties of the observable which are directly related to interference, in a second-quantization framework. In Sec. 4, we review the main results on the typicality of interference between two expanding Gaussian modes, which constitute a realistic model of a BEC interferometry experiment. In Sec. 5, we consider the role of the interaction among particles and write down a simple Hamiltonian model, and in Sec. 6, we show how an initial coherent state evolves under this Hamiltonian. Finally, in Sec. 7, we show how this simple physical mechanism yields a dynamical randomization of the phases in the two-mode Fock basis.

2. Distribution of Initial States

We consider a typical experimental setup of BEC interferometry: A condensate is distributed among two orthogonal modes, $\psi_a(\boldsymbol{r})$ and $\psi_b(\boldsymbol{r})$, which are usually spatially separated at some initial time. Then the atomic clouds are let to expand, overlap, and (possibly) interfere.

Let us assume that the total number of bosons N is fixed. A useful basis for such a system is given by two-mode Fock states

$$|\ell\rangle := \left| \left(\frac{N}{2}+\ell\right)_a, \left(\frac{N}{2}-\ell\right)_b \right\rangle = \frac{1}{\sqrt{\left(\frac{N}{2}+\ell\right)!\,\left(\frac{N}{2}-\ell\right)!}} (\hat{a}^\dagger)^{\frac{N}{2}+\ell} (\hat{b}^\dagger)^{\frac{N}{2}-\ell} |\Omega\rangle, \qquad (1)$$

with $-N/2 \leq \ell \leq N/2$, in which the two modes $\psi_a(\boldsymbol{r})$ and $\psi_b(\boldsymbol{r})$ are orthonormal, and have well-defined occupation numbers. We assume that N is even for simplicity. The mode operators,

$$\hat{a} = \int d\boldsymbol{r}\ \psi_a^*(\boldsymbol{r})\hat{\Psi}(\boldsymbol{r}), \quad \hat{b} = \int d\boldsymbol{r}\ \psi_b^*(\boldsymbol{r})\hat{\Psi}(\boldsymbol{r}), \tag{2}$$

annihilate the vacuum state $|\Omega\rangle$ and satisfy the canonical commutation relations $[\hat{a}, \hat{a}^\dagger] = [\hat{b}, \hat{b}^\dagger] = 1$, all the operators of mode a commuting with those of mode b. Here $\hat{\Psi}(\boldsymbol{r})$ is the bosonic field operator, satisfying the canonical commutation relations $[\hat{\Psi}(\boldsymbol{r}), \hat{\Psi}^\dagger(\boldsymbol{r}')] = \delta(\boldsymbol{r} - \boldsymbol{r}')$, etc. The number operators $\hat{N}_a = \hat{a}^\dagger \hat{a}$ and $\hat{N}_b = \hat{b}^\dagger \hat{b}$ count the numbers of particles in the two modes.

The crucial assumption[25] is that the initial state of the two-mode system is randomly picked from the subspace spanned by the Fock states with $|\ell| < n/2$,

$$\mathcal{H}_n = \mathrm{span}\{|\ell\rangle \,|{-n/2} < \ell < n/2\}, \tag{3}$$

with $0 < n \leq N+1$, where n is odd for simplicity, and the microcanonical density matrix reads

$$\hat{\varrho}_n = \frac{1}{n} \sum_{|\ell|<n/2} |\ell\rangle\langle\ell|. \tag{4}$$

The case $n = 1$ was studied by a number of authors,[16–18,20,31–34] while we are more interested in the large-n case. It is not harmful to think of the "natural" situation $n = O(\sqrt{N})$, but we shall work in full generality, with an arbitrary $n = o(N)$. Surprisingly, interference turns out to be robust[25] against the stronger scaling $n = o(N)$, which includes, for example, $n \sim N/\log N$.

A general pure state $|\Phi_N\rangle$ of the system drawn from the (unit sphere) of the subspace $\mathcal{H}_n$ can be expanded in the Fock basis (1) as:

$$|\Phi_N\rangle = \sum_{|\ell|<n/2} z_\ell |\ell\rangle, \quad \sum_{|\ell|<n/2} |z_\ell|^2 = 1, \tag{5}$$

since $z_\ell = 0$ for $|\ell| \geq n/2$. The coefficients z_ℓ for $|\ell| < n/2$ are randomly sampled from the surface of the $2n$-dimensional unit sphere $\sum_\ell |z_\ell|^2 = 1$.

The assumption of *uniform* sampling is a simplifying one: the number of states that are actually involved in the description and their amplitude will depend on the experimental procedure and the way the two BEC clouds are created.[35] Due to this assumption, the quadratic *statistical* average over all experimental runs (5) reads

$$\overline{z_{\ell_1}^* z_{\ell_2}} = \frac{1}{n} \delta_{\ell_1,\ell_2}, \tag{6}$$

while the average of the coefficients themselves, as well as all the quantities that depend on the phases of the coefficients, will vanish.

In a given run, with state $|\Phi_N\rangle$, a quantum observable $\hat{A}$ has expectation value

$$A_{\Phi_N} = \langle\Phi_N|\hat{A}|\Phi_N\rangle. \tag{7}$$

Its statistical average over all experimental runs, described by the uniform ensemble (5), is

$$\overline{A} := \overline{\langle\Phi_N|\hat{A}|\Phi_N\rangle} = \mathrm{Tr}(\hat{\varrho}_n\hat{A}) = A_{\varrho_n}. \tag{8}$$

There are two distinct fluctuations that characterize a given observable: (i) the *statistical fluctuations* of A_{Φ_N} over the experimental runs, quantified by the statistical variance

$$(\delta A)^2 := \overline{A^2} - \overline{A}^2 = \overline{\langle\Phi_N|\hat{A}|\Phi_N\rangle^2} - \overline{\langle\Phi_N|\hat{A}|\Phi_N\rangle}^2; \tag{9}$$

(ii) the *quantum fluctuations* of observable $\hat{A}$ in a single run, quantified by the observable $(\Delta\hat{A})^2 = (\hat{A} - A_{\Phi_N})^2$. The statistical average of its expectation value in state $|\Phi_N\rangle$ reads

$$\overline{(\Delta A)^2} := \overline{\langle\Phi_N|\hat{A}^2|\Phi_N\rangle} - \overline{\langle\Phi_N|\hat{A}|\Phi_N\rangle^2}. \tag{10}$$

Computations of (9) and (10) both involve the quartic average[36] $\overline{z^*_{\ell_1}z^*_{\ell_2}z_{\ell_3}z_{\ell_4}}$. Notice, however, that their sum involves only quadratic averages, and is in fact given by the quantum mechanical variance of $\hat{A}$ in the microcanonical state ϱ_n in (4):

$$\overline{(\Delta A)^2} + (\delta A)^2 = (\Delta A)^2_{\varrho_n} = \mathrm{Tr}(\hat{\varrho}_n\hat{A}^2) - \mathrm{Tr}(\hat{\varrho}_n\hat{A})^2. \tag{11}$$

A few comments are in order. If the initial state is sampled from the degenerate distribution with $n = 1$ (which is in fact deterministic and concentrated on the single balanced Fock state), the average quantum variance $\overline{(\Delta A)^2}$ coincides with the quantum variance of $|\ell = 0\rangle$, while, obviously, $(\delta A)^2 = 0$. In such a case, the same state is prepared in every run (which requires a very careful preparation procedure and is a somewhat unrealistic assumption for the experiments performed so far). On the other hand, if the ensemble is made up of eigenstates of the observable $\hat{A}$, then the quantum fluctuations vanish, $\overline{(\Delta A)^2} = 0$, and the only contribution to (11) comes from the statistical fluctuations $(\delta A)^2$, that differentiate individual runs. An observable is *typical* if $(\delta A)^2 = o(\overline{A}^2)$, and is *stable* at each run if $\overline{(\Delta A)^2} = o(\overline{A}^2)$.

In general, different fluctuations are present in a given experiment. We analyzed the interference of a two-mode Bose–Einstein system according to these ideas and showed that some features of the interference pattern (such as its period and its fringe contrast) are *robust* against both the afore-mentioned fluctuations,[25] and thus $(\Delta A)^2_{\varrho_n} = o(\overline{A}^2)$. We shall summarize the main results in the following sections and shall comment on the role of $(\Delta A)^2_{\varrho_n}$ for an interesting observable, the power spectrum of particle density.[34]

3. Observables Related to Interference

Since we are interested in the quantities that are related to interference, we will focus on those observables associated with the spatial distribution of particles.[31,34,37–40] In this section, we will review the relevant averages in the general case, postponing quantitative considerations to the following section. In the second-quantization formalism, the spatial density is represented by the operator

$$\hat{\rho}(\boldsymbol{r}) = \hat{\Psi}^{\dagger}(\boldsymbol{r})\,\hat{\Psi}(\boldsymbol{r}), \tag{12}$$

whose Fourier transform reads

$$\widehat{\hat{\rho}}(\boldsymbol{k}) := \mathcal{F}[\hat{\rho}](\boldsymbol{k}) = \int d\boldsymbol{r}\, e^{-i\boldsymbol{k}\cdot\boldsymbol{r}}\hat{\rho}(\boldsymbol{r}). \tag{13}$$

Expanding the field operators and taking the expectation value (8), one finds that the average density

$$\overline{\rho(\boldsymbol{r})} = \overline{\langle \Phi_N|\hat{\rho}(\boldsymbol{r})|\Phi_N\rangle} = \frac{N}{2}\left(\rho_a(\boldsymbol{r}) + \rho_b(\boldsymbol{r})\right), \quad \text{with } \rho_{a,b}(\boldsymbol{r}) := |\psi_{a,b}(\boldsymbol{r})|^2, \tag{14}$$

is merely the sum of the particle densities in the two modes, with no interference between them. Clearly, this property holds also for the Fourier transform. This result apparently contrasts with experimental observation, as interference is present even if no phase coherence between the particles in the two modes exists. However, the average (14) cannot give sufficient information on the result of a *single* experimental run, since its fluctuations are very large.

On the other hand, the outcome of a single run can be inferred, within a controlled degree of approximation, from the study of the *density power spectrum*, i.e. the square modulus of its Fourier transform[31,34,37–40]:

$$\hat{R}(\boldsymbol{k}) := \widehat{\hat{\rho}}^{\dagger}(\boldsymbol{k})\,\widehat{\hat{\rho}}(\boldsymbol{k}) = \hat{r}(\boldsymbol{k}) + \hat{N}, \tag{15}$$

$$\hat{r}(\boldsymbol{k}) := \int d\boldsymbol{r}\, d\boldsymbol{r}' e^{-i\boldsymbol{k}\cdot(\boldsymbol{r}-\boldsymbol{r}')}\hat{\Psi}^{\dagger}(\boldsymbol{r})\,\hat{\Psi}^{\dagger}(\boldsymbol{r}')\,\hat{\Psi}(\boldsymbol{r}')\,\hat{\Psi}(\boldsymbol{r}). \tag{16}$$

Observe that all states $|\Phi_N\rangle$ in (6) are eigenstates of the total number operator $\hat{N}$ belonging to the eigenvalue N, that is fixed, which makes the role of the last addendum in (15) immaterial. Notice also that the power spectrum $\hat{R}(\boldsymbol{k})$ is the Fourier transform of the density autocorrelation function

$$\hat{C}(\boldsymbol{r}) = \int d\boldsymbol{r}'\hat{\rho}(\boldsymbol{r}')\hat{\rho}(\boldsymbol{r}+\boldsymbol{r}'). \tag{17}$$

Under specific assumptions on the values of N and n in (3), we will show that fluctuations around the average value

$$\overline{R(\boldsymbol{k})} = \mathrm{Tr}(\hat{\varrho}_n\hat{R}(\boldsymbol{k})) \tag{18}$$

are negligible.

The observable $\hat{r}(\boldsymbol{k})$ can be expanded in the mode operators as:

$$\begin{aligned}\hat{r}(\boldsymbol{k}) = {} & |\tilde{\rho}_a(\boldsymbol{k})|^2 \hat{N}_a(\hat{N}_a - 1) + |\tilde{\rho}_b(\boldsymbol{k})|^2 \hat{N}_b(\hat{N}_b - 1) \\ & + (\tilde{\rho}_a^*(\boldsymbol{k})\tilde{\rho}_b(\boldsymbol{k}) + \tilde{\rho}_b^*(\boldsymbol{k})\tilde{\rho}_a(\boldsymbol{k}) + |\tilde{\rho}_{ba}(\boldsymbol{k})|^2 + |\tilde{\rho}_{ab}(\boldsymbol{k})|^2)\hat{N}_a\hat{N}_b \\ & + [(\tilde{\rho}_b(-\boldsymbol{k})\tilde{\rho}_{ba}(\boldsymbol{k}) + \tilde{\rho}_b(\boldsymbol{k})\tilde{\rho}_{ba}(-\boldsymbol{k}))\hat{N}_b\hat{b}^\dagger\hat{a} \\ & + (\tilde{\rho}_{ba}(-\boldsymbol{k})\tilde{\rho}_a(\boldsymbol{k}) + \tilde{\rho}_{ba}(\boldsymbol{k})\tilde{\rho}_a(-\boldsymbol{k}))\hat{b}^\dagger\hat{a}\hat{N}_a \\ & + \tilde{\rho}_{ba}(-\boldsymbol{k})\tilde{\rho}_{ba}(\boldsymbol{k})(\hat{b}^\dagger)^2\hat{a}^2 + \text{h.c.}] + \text{other modes},\end{aligned} \tag{19}$$

with $\tilde{\rho}_{ba}(\boldsymbol{k}) := \mathcal{F}[\psi_b^*\psi_a](\boldsymbol{k})$. Due to the uniform sampling (5) in $\mathcal{H}_n$, only the first three operators in (19), which have diagonal matrix elements in the Fock basis, yield non-vanishing contributions to the ensemble average of $\hat{R}(\boldsymbol{k})$. The final result reads

$$\overline{R(\boldsymbol{k})} = \overline{r(\boldsymbol{k})} + N = \frac{N^2}{4}(|\tilde{\rho}_a(\boldsymbol{k}) + \tilde{\rho}_b(\boldsymbol{k})|^2 + |\tilde{\rho}_{ba}(\boldsymbol{k})|^2 + |\tilde{\rho}_{ab}(\boldsymbol{k})|^2) + O(N, n^2), \tag{20}$$

in which the Fourier transforms of $\psi_b^*\psi_a$, directly related to interference, appear. (Remember that we always assume $n = o(N)$.)

We now estimate the fluctuations of $\hat{R}$ according to the philosophy outlined in the previous section. In order to estimate the fluctuations of $\hat{R}(\boldsymbol{k})$ around its average and prove that they are small in the large-N limit, we shall consider the covariance

$$\begin{aligned}(\Delta R)^2_{\varrho_n}(\boldsymbol{k}, \boldsymbol{k}') = {} & \mathrm{Tr}(\hat{\varrho}_n\hat{R}(\boldsymbol{k})\hat{R}(\boldsymbol{k}')) - \mathrm{Tr}(\hat{\varrho}_n\hat{R}(\boldsymbol{k}))\mathrm{Tr}(\hat{\varrho}_n\hat{R}(\boldsymbol{k}')) \\ = {} & \mathrm{Tr}(\hat{\varrho}_n\hat{R}(\boldsymbol{k})\hat{R}(\boldsymbol{k}')) - \overline{r(\boldsymbol{k})}\cdot\overline{r(\boldsymbol{k}')}.\end{aligned} \tag{21}$$

It involves (diagonal) matrix elements of the four-particle correlation function $\prod_{i=1}^4 \hat{\Psi}^\dagger(\boldsymbol{r}_i)\prod_{i=1}^4 \hat{\Psi}(\boldsymbol{r}_i)$. In the following section, we will analyze an experimentally relevant case in which the distribution of $R(\boldsymbol{k})$ displays sharp peaks that provide information on the interference pattern in each experimental run, with fluctuations being negligible in proper ranges of N and n.

4. Typical Interference of Expanding Gaussian Modes

In the light of the general results on the density power spectrum $\hat{R}(\boldsymbol{k})$ and its fluctuations, we will review in this section the properties of a realistic model, describing a physical situation that is close to experimental implementation. The cold atoms are initially trapped in two Gaussian clouds by an external double-well potential. The distance between the peaks of the distributions is significantly larger than their widths, so that the initial wave packets do not overlap. The trap is then released and the clouds expand freely until they overlap and interfere. We will explicitly consider the time evolution of the system in one spatial dimension, for simplicity: if scattering between the particles in the condensates is neglected, the time dependence can be evaluated by observing that the correlation functions at time t are obtained by replacing the initial modes $\psi_{a,b}(x)$ with their time-evolved counterparts

$$\psi_{a,b}(x,t) = \exp\left(\frac{i\hbar t}{2m}\frac{\partial^2}{\partial x^2}\right)\psi_{a,b}(x), \tag{22}$$

with

$$\psi_a(x) = \frac{1}{\pi^{1/4}\sigma^{1/2}}\, e^{-(x+\alpha)^2/2\sigma^2}, \quad \psi_b(x) = \frac{1}{\pi^{1/4}\sigma^{1/2}}\, e^{-(x-\alpha)^2/2\sigma^2}, \tag{23}$$

where σ is the width of the Gaussians and α is the half distance between their maxima, chosen large enough in order to ensure that $\psi_{a,b}$ are approximately orthogonal.

A straightforward calculation yields[25]

$$\begin{aligned}(\Delta R)^2_{\varrho_n}(k,k';t) = {} & N^3 C_{3,0}(k,k';t) + Nn^2 C_{1,2}(k,k';t) \\ & + n^4 C_{0,4}(k,k';t) + n^3 C_{0,3}(k,k';t) + O(N^2),\end{aligned} \tag{24}$$

where the coefficients $C_{i,j}$ depend on the structure of the modes, but neither on the number of particles N, nor on the dimension n of the sampled Hilbert subspace.

Equation (24) shows that fluctuations are $o(N^4)$ when $n = o(N)$. This implies that if $n = o(N)$ (i.e. $n/N \to 0$ for $N \to \infty$) fluctuations around the average $\overline{R}$ in (24) in different experimental runs are negligible, and the distribution of the measured values of $\hat{R}$ is peaked around its most probable value. These results prove that interference is typical, and occurs for the overwhelming majority of wave functions of the condensate when $n = o(N)$.

We observe that similar conclusions are obtained when one deals with plane waves rather than Gaussian modes,[25] the only difference being in the coefficients $C_{i,j}$ in Eq. (24). Presumably, the dependence on N and n will not change for a wide range of mode functions. In this sense, our conclusions are of general validity.

5. The Self-Interacting Gas

The results reviewed in the previous sections were obtained by averaging over an ensemble of states. It is not immediate to relate these results to an experiment, since one should introduce a mechanism to sample the random states according to the desired distribution. We will show in the following that the randomization of the *phases* in the Fock basis emerges in a natural and straightforward way, once interparticle scattering is considered.

In a classical double-slit experiment, first-order interference is observable if the relative phase ϕ between the incident waves at each slit does not vary over time. The corresponding case for a condensate is that of a two-mode *coherent* state (see Eq. (29)–(30) in the following), in which all the N particles are in the same superposition of mode wave functions. A first-order interference pattern can be observed in a coherent state, with the same offset ϕ at each experimental run.

It is not obvious that a coherent state is created when two (independent) Bose-Einstein condensates are prepared. Nevertheless, we shall now scrutinize the evolution of a coherent state when the Bose gas is self-interacting. In such a case, the phases in the Fock basis expansion become (pseudo)random after an initial transient, whose duration vanishes in the $N \to \infty$ limit. We will show that this behavior is closely related to a loss of coherence between the two modes, which leads to the disappearence of the first-order pattern after the initial transient. This is also related to the general theory of the Josephson effect[5] and spin squeezing.[41] Our previous results ensure, on the other hand, that an interference pattern can be observed also in this case, despite its offset fluctuates over time and experimental runs.

Let us consider a Bose system with particles distributed in two *spatially separated* orthonormal modes ψ_a and ψ_b, whose supports S_a and S_b do not overlap. Assume that the energies of a single particle in each mode be equal, so that we can set them equal to zero for convenience, and that the tunneling between the two modes is negligible. If we also assume that other modes are made inaccessible (e.g. by a large energetic separation), the two-body contact-interaction term in the Hamiltonian reads

$$\begin{aligned} \hat{H}_{\text{int}} &= \frac{g}{2} \int d\boldsymbol{r}\, \hat{\Psi}^\dagger(\boldsymbol{r})\, \hat{\Psi}^\dagger(\boldsymbol{r})\, \hat{\Psi}(\boldsymbol{r})\, \hat{\Psi}(\boldsymbol{r}) \\ &\simeq \frac{g}{2} \left(\int_{S_a} d\boldsymbol{r} \rho_a^2(\boldsymbol{r}) \right) \hat{N}_a(\hat{N}_a - 1) + \frac{g}{2} \left(\int_{S_b} d\boldsymbol{r} \rho_b^2(\boldsymbol{r}) \right) \hat{N}_b(\hat{N}_b - 1), \end{aligned} \tag{25}$$

where the coupling constant g is determined at the lowest order by the scattering length a_s through $g = 4\pi\hbar^2 a_s/m$, and the products of a and b mode operators do not appear because the supports of the modes have no overlap. If the integrals appearing in (25) are equal (e.g. if the mode density profiles are related by translation and/or reflection), the Hamiltonian reduces to

$$\begin{aligned} \hat{H}_{\text{int}} &= \frac{\tilde{g}}{2} \left[\hat{N}_a{}^2 + \hat{N}_b{}^2 - (\hat{N}_a + \hat{N}_b) \right] \\ &= \frac{\tilde{g}}{2} \left[\frac{(\hat{N}_a - \hat{N}_b)^2}{2} + \frac{(\hat{N}_a + \hat{N}_b)^2}{2} - (\hat{N}_a + \hat{N}_b) \right], \end{aligned} \tag{26}$$

where $\tilde{g} := g \int_{S_a} d\boldsymbol{r} \rho_a^2(\boldsymbol{r})$. Since $\hat{N}_a + \hat{N}_b = \hat{N}$ is a constant of motion and we are going to consider states with a fixed number of particles N, distributed among the two modes, the only part of the Hamiltonian which is relevant to the evolution of a state $|\Phi_N\rangle$ is

$$\hat{h} = \tilde{g}(\delta\hat{N})^2, \quad \text{with } \delta\hat{N} = \frac{\hat{N}_a - \hat{N}_b}{2}. \tag{27}$$

By definition, the N-particle two-mode Fock basis (1) satisfies

$$\delta\hat{N}|\ell\rangle = \ell|\ell\rangle. \tag{28}$$

6. Dynamics and Typicality

Let us consider an initial coherent state,

$$|\Psi_0\rangle = \frac{1}{\sqrt{N!}}\left(\frac{\hat{a}^\dagger + \hat{b}^\dagger}{\sqrt{2}}\right)^N |\Omega\rangle = \frac{1}{2^{N/2}} \sum_{\ell=-N/2}^{N/2} \binom{N}{N/2+\ell}^{\frac{1}{2}} |\ell\rangle, \tag{29}$$

in which all the particles are created in the wave function $[\psi_a(\boldsymbol{r}) + \psi_b(\boldsymbol{r})]/\sqrt{2}$. Once the initial wave packets are let to expand and *overlap*, this state, along with all the states

$$|\varphi\rangle = \frac{1}{\sqrt{N!}}\left(\frac{e^{i\varphi/2}\hat{a}^\dagger + e^{-i\varphi/2}\hat{b}^\dagger}{\sqrt{2}}\right)^N |\Omega\rangle = \frac{1}{2^{N/2}} \sum_{\ell=-N/2}^{N/2} \binom{N}{N/2+\ell}^{\frac{1}{2}} e^{i\ell\varphi}|\ell\rangle, \tag{30}$$

displays first-order interference, appearing in the expectation value $\langle\varphi|\hat{\rho}(\boldsymbol{r},t)|\varphi\rangle$ with maximal visibility, since the relative phase between the two modes is fixed and the modes are equally populated on average. The coherent states (30), called phase states,[7,19,20,24] which are relevant to describe interference, do not form a basis. Their overlap reads

$$\langle\varphi|\varphi'\rangle = \left(\cos\frac{\varphi-\varphi'}{2}\right)^N \tag{31}$$

and is characterized for large N by a sharp peak around $\varphi - \varphi' = 0$, whose width is $O(N^{-1/2})$.

Even if all the coefficients of the states (29) and (30) in the Fock basis are non-vanishing, the presence of the binomial coefficient implies that for large N the states can be very well approximated by truncating the sum at $|\ell| < \ell_{\max} = O(N^{1/2})$: The approximate states thus belong to $\mathcal{H}_{2\ell_{\max}}$ (see Eq. (3)). The evolution of the initial state (29) generated by the Hamiltonian (27) reads

$$|\Psi(t)\rangle = \sum_{\ell=-N/2}^{N/2} \binom{N}{N/2+\ell}^{\frac{1}{2}} \frac{e^{-i\ell^2\tilde{g}t}}{2^{N/2}}|\ell\rangle. \tag{32}$$

In general, the evolved state at $t > 0$ is no longer a coherent state of the form (30): The delicate phase relation between the amplitudes in the Fock basis breaks due to the time-dependent phase factors, which are quadratic in the imbalance ℓ. This behavior produces a pseudo-randomization for irrational values of $\tilde{g}t/\pi$, which simulates the random phase sampling in the statistical ensemble for a fixed distribution of the imbalances. A detailed analysis of this aspect will be presented in the following.

The loss of relative coherence can be quantified by studying the squared component of the state $|\Psi(t)\rangle$ along the general coherent state $|\varphi\rangle$:

$$P_\varphi(t) = |\langle\varphi|\Psi(t)\rangle|^2 = \left|\frac{1}{2^N}\sum_{\ell=-N/2}^{N/2}\binom{N}{N/2+\ell} e^{-i\ell\varphi - i\ell^2\tilde{g}t}\right|^2. \tag{33}$$

A peaked distribution around one value of the relative phase φ indicates a high degree of coherence, and thus a large visibility in the first-order interference. On the other hand, an almost uniform value of (33) in $(-\pi, \pi]$ indicates that very small phase coherence between the particles in the two modes is present, and the offset of the interference fringes randomly fluctuates from run to run, leading to the disappearance of first-order interference effects. The relative phase distribution of the initial state (29) is peaked around $\varphi = 0$. Notice that the peak has a finite width, since each coherent state can be expressed as a linear superposition of the others. The peak becomes sharper as N increases, with a standard deviation

$$\sigma_\varphi(0) = \sqrt{\int_{-\pi}^{+\pi} d\varphi \varphi^2 P_\varphi(0) \Big/ \int_{-\pi}^{+\pi} d\varphi P_\varphi(0)} = \sqrt{\frac{2}{N}}. \tag{34}$$

As the system evolves, the initial value of σ_φ becomes negligible, as the standard deviation increases linearly in time, like

$$\sigma_\varphi(t) \simeq \sqrt{N/2}\,\tilde{g}t. \tag{35}$$

This result can be immediately obtained by a Gaussian approximation of the binomial coefficients,

$$\frac{1}{2^N}\binom{N}{N/2+\ell} \sim \sqrt{\frac{2}{\pi N}} e^{-\frac{2}{N}\ell^2}, \tag{36}$$

for $N \to \infty$. At time $t_* = 2\pi/\tilde{g}\sqrt{2N}$, one expects that the state is spread over all possible values of the relative phase. This does not prevent coherence to be recovered at a subsequent time: indeed the state is again perfectly coherent at $t = \pi/\tilde{g}$, because $|\Psi(\pi/\tilde{g})\rangle = |\varphi = \pi\rangle$, and returns to the initial state $|\varphi = 0\rangle$ after the recurrence time $t = t_r := 2\pi/\tilde{g}$.

7. Phase Randomization

Let us now discuss the phase randomization process which involves the coefficients of $|\Psi(t)\rangle$ in the expansion (32): their phases are

$$f_\ell(t) := \tilde{g}t\ell^2 \bmod 2\pi. \tag{37}$$

Can the sequence $\{f_\ell\}_{|\ell|\le N/2}$ mimic a random sequence, sampled from a uniform distribution in $[0, 2\pi]$, for some time t? To address this question, one can analyze a quantity which is common in testing pseudorandom numbers, namely the autocorrelation between nearest phases

$$C(t) = \frac{(N+1)\sum_\ell f_\ell(t) f_{\ell+1}(t) - [\sum_\ell f_\ell(t)]^2}{(N+1)\sum_\ell f_\ell^2(t) - [\sum_\ell f_\ell(t)]^2}, \tag{38}$$

which is expected to vanish for a truly random sequence of independent phases. At the initial time, the values of the phases for adjacent ℓ's are strongly correlated, since

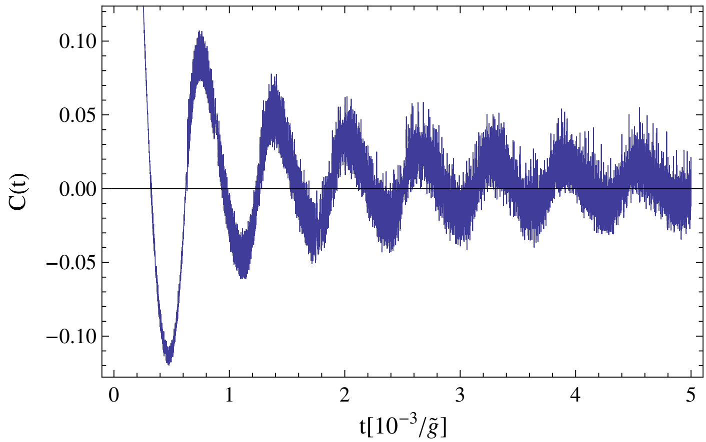

Fig. 1. Autocorrelation $C(t)$, defined in (37) and (38), of the sequence of phases $f_\ell(t)$ in the case $N = 10^4$. Though very rapidly variating, the function is analytic for all finite N. The spacing between points in the horizontal axis is $t = 10^{-6}/\tilde{g}$. Recall that at the initial time the sequence of coefficients is perfectly correlated ($C(0) = 1$, not shown in the plot).

$C(0) = 1$. The autocorrelation reduces as time increases: for $N = 10^4$, its value typically drops down to $|C(t)| \lesssim 0.05$ at $\tilde{g}t \simeq 2 \cdot 10^{-3}$, with oscillations around zero (see Fig. 1). An exception to this behavior occurs when $\tilde{g}t/\pi$ is a rational number: in this case, phases are not uniformly distributed in $[0, 2\pi]$, since they can assume only a finite set of values. In Fig. 2, the projection $P_\varphi(t)$ of the state $|\Psi(t)\rangle$ on the coherent state with relative phase φ (see (33)) is plotted as a function of φ, in parallel with a scatter plot of the phases $f_\ell(t)$.

The plot in Fig. 2(a) shows a distribution P_φ evaluated at $\tilde{g}t = 10^{-6}$, which is still peaked around $\varphi = 0$, indicating a good degree of coherence (left panel). On the other hand, the phases f_ℓ of adjacent Fock coefficients are manifestly correlated, with $C(10^{-6}/\tilde{g}) = 0.997$ (right panel).

At time $\tilde{g}t_* = \sqrt{2/N}\pi \simeq 0.044$, the function P_φ spreads over the whole interval $(-\pi, \pi]$, as shown in Fig. 2(b) (left panel). No correlations manifestly emerge between the phases of the coefficients, which appear to be (almost) uniformly scattered (right panel). This observation is confirmed by the small value of the autocorrelation $C(0.044/\tilde{g}) = -3.4 \cdot 10^{-3}$ (not shown in Fig. 1, where shorter times $t \leq 5 \cdot 10^{-3}/\tilde{g}$ are displayed).

In Figs. 2(c) and 2(d), two different situations that can occur at large times are presented (both cases are not shown in Fig. 1, that displays times of order $t \sim 10^{-3}/\tilde{g}$). When $\tilde{g}t/\pi$ is irrational, Fig. 2(c), the phases of the coefficients are pseudorandom $[C(1.5/\tilde{g}) \simeq 10^{-2}]$ (left panel), and the relative phase distribution tends to fill the interval $(-\pi, \pi]$ uniformly (right panel). On the other hand, when $\tilde{g}t/\pi = p/q$ is rational, Fig. 2(d), the phases of the coefficients become periodic, with

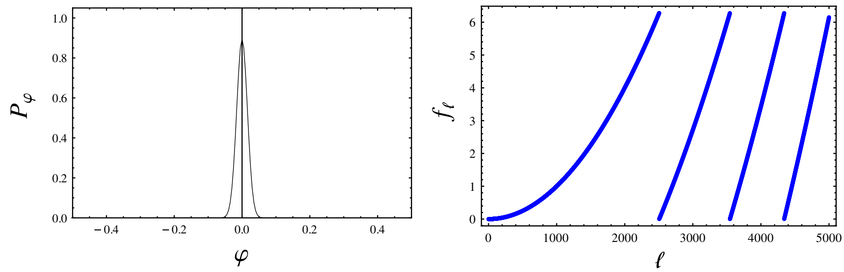

(a) $\tilde{g}t = 10^{-6}$

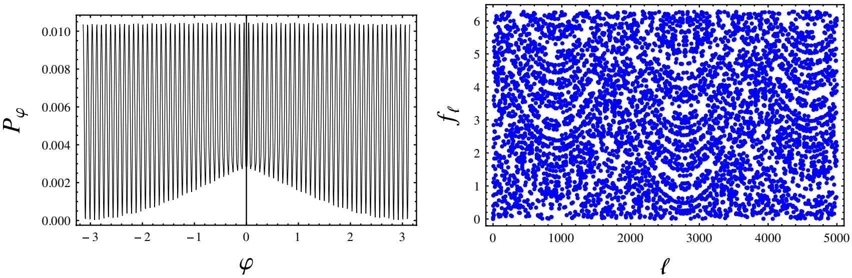

(b) $\tilde{g}t = 0.044$

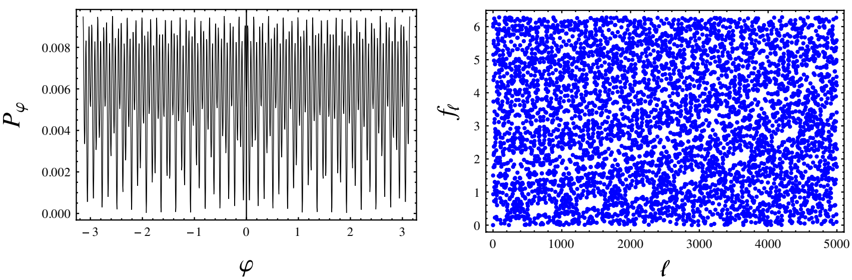

(c) $\tilde{g}t = 1.5$

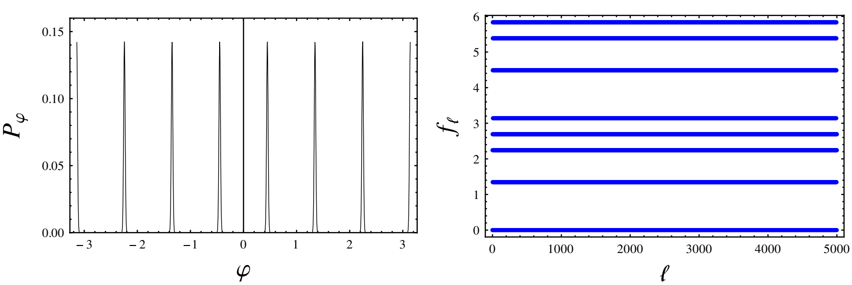

(d) $\tilde{g}t = 5\pi/7$

Fig. 2. The two columns display in parallel, for different times, the behavior of the squared component $P_\varphi(t)$ of $|\Psi(t)\rangle$ along the coherent state defined by phase φ (left panels), and the distribution of the phases $f_\ell(t)$ of the coefficients in the Fock basis (right panels) (see (33)–(37)). The loss of the initial coherence from (a) to (b) is due to the randomization of the phases. The last two plots refer to long-time cases in which (c) there is no coherence and (d) partial coherence is recovered.

period q if p is even and $2q$ if p is odd: No randomization occurs in this case, and the state of the system appears as a superposition of a finite number of coherent states (left panel). The phases are very correlated (right panel).

Let us finally remark that full correlation among the coefficients is recovered, together with coherence, when $t = t_r/2$ (the recurrence time defined at the end of Sec. 6). Our case study shows how the randomization of the coefficients and the loss of coherence between the two modes are strictly correlated. If one observes the state of the system at a generic time t in $[0, t_r]$, in the vast majority of cases the phases of the coefficients behave as if they were sampled from a random distribution. One can thus expect in this case that the typical properties of the system are captured by the average over a distribution of states with random phases in the Fock basis coefficients.

It should be observed that in the case here considered there is no mechanism that yields a randomization of the *amplitudes* of the coefficients. Of course, it is possible to conceive several physical situations that do not preserve the imbalance distribution ℓ, and randomize also the amplitudes. However, the results of the previous section crucially depend only on the randomness of the phases, and seem to indicate that one should expect only slightly quantitative differences if the amplitudes were sampled differently from the uniform sampling (5).

8. Conclusion

Typicality is a fecund concept in modern statistical mechanics. Typical phenomena characterize physical situations with overwhelming probability. We have shown in Ref. 25 and in this paper that the interference of two *independently prepared* BECs is typical, namely (almost) always occurs when two BECs are created and let to interfere. This interference is not of first order. We therefore looked at the relative phase of the condensates in order to elucidate its randomization mechanism.

We showed that self-interaction (accounting for two-body scattering processes) within the condensates yields such phase randomization and makes first-order interference vanish. After a certain time, that is inversely proportional to the interaction strength, the relative phase is randomized. However, an interference pattern will still be observed, as a consequence of typicality. The interplay between the absence of first-order interference and the (observable and experimentally observed) presence of second-order interference is an interesting phenomenon, that characterizes the physics of BECs.

References

1. A. S. Parkins and D. F. Walls, *Phys. Rep.* **303** (1998) 1.
2. F. Dalfovo, S. Giorgini, L. P. Pitaevskii and S. Stringari, *Rev. Mod. Phys.* **71** (1999) 463.
3. A. J. Leggett, *Rev. Mod. Phys.* **73** (2001) 307.
4. I. Bloch, J. Dalibard and W. Zwerger, *Rev. Mod. Phys.* **80** (2008) 885.

5. L. Pitaevskii and S. Stringari, *Bose–Einstein Condensation* (Oxford University Press, Oxford, 2003).
6. C. J. Pethick and H. Smith, *Bose–Einstein Condensation in Dilute Gases*, 2nd edn. (Cambridge University Press, Cambridge, 2008).
7. A. J. Leggett, *Quantum Liquids: Bose Condensation and Cooper Pairing in Condensed-Matter Systems* (Oxford University Press, Oxford, 2006).
8. M. R. Andrews, C. G. Townsend, H.-J. Miesner, D. S. Durfee, D. M. Kurn and W. Ketterle, *Science* **275** (1997) 637.
9. P. A. M. Dirac, *The Principles of Quantum Mechanics*, 4th edn. (Oxford University Press, Oxford, 1958).
10. R. Feynman, R. Leighton and M. Sand, *The Feynman Lectures on Physics*, Vol. 3 (Addison Wesley Longman, Reading, MA, 1970).
11. M. Namiki and S. Pascazio, *Phys. Rep.* **232** (1993) 301.
12. M. Namiki, S. Pascazio and H. Nakazato, *Decoherence and Quantum Measurements* (World Scientific, Singapore, 1997).
13. R. Hanbury Brown and R. Q. Twiss, *Nature (London)* **177** (1956) 27.
14. R. Hanbury Brown and R. Q. Twiss, *Nature (London)* **178** (1956) 1046.
15. L. Mandel and E. Wolf, *Optical Coherence and Quantum Optics* (Cambridge University Press, Cambridge, 1995).
16. J. Javanainen and S. M. Yoo, *Phys. Rev. Lett.* **76** (1996) 161.
17. J. I. Cirac, C. W. Gardiner, M. Naraschewski and P. Zoller, *Phys. Rev. A* **54** (1996) 3714(R).
18. T. Wong, M. J. Collett and D. F. Walls, *Phys. Rev. A* **54** (1996) 3718(R).
19. K. Mølmer, *Phys. Rev. A* **55** (1997) 3195.
20. Y. Castin and J. Dalibard, *Phys. Rev. A* **55** (1997) 4330.
21. K. Góral, M. Gajda and K. Rzażewski, *Phys. Rev. A* **66** (2002) 051602(R).
22. S. Anderloni, F. Benatti, R. Floreanini and A. Trombettoni, *J. Phys. A: Math. Theor.* **42** (2009) 035306.
23. F. Benatti, R. Floreanini and G. G. Guerreschi, *Phys. Lett. A* **373** (2009) 3516.
24. A. J. Leggett and F. Sols, *Found. Phys.* **21** (1991) 353.
25. P. Facchi, H. Nakazato, S. Pascazio, F. V. Pepe and K. Yuasa, *Phys. Rev. A* **89** (2014) 063625.
26. T. Schumm, S. Hofferberth, L. M. Andersson, S. Wildermuth, S. Groth, I. Bar-Joseph, J. Schmiedmayer and P. Krüger, *Nature Phys.* **1** (2005) 57.
27. S. Hofferberth, I. Lesanovsky, B. Fischer, J. Verdu and J. Schmiedmayer, *Nat. Phys.* **2** (2006) 710.
28. S. Hofferberth, I. Lesanovsky, B. Fischer, T. Schumm and J. Schmiedmayer, *Nature (London)* **449** (2007) 324.
29. S. Hofferberth, I. Lesanovsky, T. Schumm, A. Imambekov, V. Gritsev, E. Demler and J. Schmiedmayer, *Nat. Phys.* **4** (2008) 489.
30. T. Langen, R. Geiger, M. Kuhnert, B. Rauer and J. Schmiedmayer, *Nat. Phys.* **9** (2013) 640.
31. A. Polkovnikov, *Europhys. Lett.* **78** (2007) 10006.
32. G. S. Paraoanu, *J. Low Temp. Phys.* **153** (2008) 285.
33. G. S. Paraoanu, *Phys. Rev. A* **77** (2008) 041605(R).
34. M. Iazzi and K. Yuasa, *Phys. Rev. A* **83** (2011) 033611.
35. K. Maussang, G. E. Marti, T. Schneider, P. Treutlein, Y. Li, A. Sinatra, R. Long, J. Estève and J. Reichel, *Phys. Rev. Lett.* **105** (2010) 080403.
36. P. Facchi, G. Florio, U. Marzolino, G. Parisi and S. Pascazio, *J. Phys. A: Math. Theor.* **43** (2010) 225303.

37. A. Polkovnikov, E. Altman and E. Demler, *Proc. Natl. Acad. Sci. USA* **103** (2006) 6125.
38. V. Gritsev, E. Altman, E. Demler and A. Polkovnikov, *Nature Phys.* **2** (2006) 705.
39. A. Imambekov, V. Gritsev and E. Demler, in *Ultra-Cold Fermi Gases*, Vol. 164 of *International School of Physics "Enrico Fermi"*, eds. M. Inguscio, W. Ketterle and C. Salomon (IOS, Amsterdam, 2007), pp. 535–606.
40. S. Ando, K. Yuasa and M. Iazzi, *Int. J. Quantum Inform.* **9** (2011) 431.
41. J. Ma, X. Wang, C. Sun and F. Nori, *Phys. Rep.* **509** (2011) 89.